Original Paper

Neonatology

Neonatology
DOI: 10.1159/000355818

Received: July 17, 2013
Accepted after revision: September 13, 2013
Published online: ■■■

Survival and Neurodevelopmental Outcome of Preterm Infants Born at 22–24 Weeks of Gestational Age

Masayuki Ochiai[a, c] Tadamune Kinjo[a, c] Yasushi Takahata[a] Mariko Iwayama[a] Takeru Abe[b] Kenji Ihara[a, c] Shouichi Ohga[c, f] Kotaro Fukushima[a, d] Kiyoko Kato[a, d] Tomoaki Taguchi[a, e] Toshiro Hara[a, c]

[a]Comprehensive Maternity and Perinatal Care Center and [b]Medical Information Center, Kyushu University Hospital, Departments of [c]Pediatrics, [d]Obstetrics and Gynecology, [e]Pediatric Surgery and [f]Perinatal and Pediatric Medicine, Graduate School of Medical Sciences, Kyushu University, Fukuoka, Japan

Key Words
Extremely premature infants · Extremely low birthweight · Mortality · Morbidity · Antenatal steroid

Abstract
Background: The limits of viability in extremely premature infants are challenging for any neonatologists in developed countries. The neurological development and growth of extremely preterm infants have come to be the emerging issue following the management in the neonatal intensive care unit. ***Objective:*** To assess potential associations between changes in practice and survival/neurodevelopmental outcome, and clinical outcomes of extremely preterm infants born at the limit of viability studied in a tertiary center. ***Study Design:*** A retrospective study enrolled 51 infants who had no congenital disorders, and were born at 22–24 weeks of gestational age (GA) in 2000–2009 in our institution. Clinical variables and interventions were studied with regard to one-year survival and developmental quotient (DQ) at 3 years of age. ***Results:*** The one-year survival rate of 24 preterm infants born in 2005–2009 (79%) was higher than that of the 27 infants born in 2000–2004 (52%, p = 0.04). Infants born after 2005 underwent less tocolysis (54 vs. 94%, p < 0.01) and more frequently antenatal steroid therapy (32 vs. 6%, p = 0.01) than those born before 2004. The post-2005 survivors (n = 19) received more frequently indomethacin therapy (89 vs. 50%, p = 0.03) and early parenteral nutrition (95 vs. 36%, p < 0.01) than the pre-2004 survivors (n = 14). There were no differences in the proportion of infants who attained a DQ of >50 at 3 years of age between pre-2004 (9/13, 69%) and post-2005 groups (10/17, 59%). Multivariate analysis indicated that extremely premature birth at GA <24 weeks was the sole critical factor for a DQ of >50 in survivors. ***Conclusions:*** The perinatal care after 2005 improved the overall survival rate, but not the neurological outcome of preterm survivors at the limit of viability. Neurodevelopmental impairments were associated with extremely premature birth at GA <24 weeks.

Introduction

Recent progress in the perinatal and neonatal care has greatly improved the prognosis of critically ill or premature newborn infants. The limits of viability in extremely premature infants are challenging for any neonatologist

KARGER

E-Mail karger@karger.com
www.karger.com/neo

1661–7800/13/0000–0000$38.00/0

Masayuki Ochiai, MD, PhD
Department of Pediatrics, Graduate School of Medical Sciences
Kyushu University 3-1-1 Maidashi, Higashi-ku
Fukuoka 812-8582 (Japan)
E-Mail ochimasa@pediatr.med.kyushu-u.ac.jp

in developed countries [1–4]. Between 2004 and 2007, the one-year survival rate of infants born at 22–26 weeks of gestational age (GA) in Sweden attained 70%, ranging from 9.8% at GA 22 to 85% at GA 26 weeks [5]. In 2005, the survival rates of Japanese infants during their stay in a neonatal intensive care unit (NICU) were 34.0, 54.2 and 76.6% in infants born at GA 22, 23, and 24 weeks, respectively [6]. On the other hand, the post-NICU neurological development and growth of extremely preterm infants have come to be the emerging issue.

Antenatal steroid therapy was reportedly associated with a significant decrease in the mortality of preterm infants born at GA 22–23 weeks [7]. This intervention was actively introduced in our tertiary center after 2005 for women at high risk of preterm delivery after GA 22 weeks. The alive-born premature infants are at high-risk for a constellation of life-threatening events including cerebral bleeding and sepsis. A small number of survivors at the limit of viability still have an increased risk of physiological and neurodevelopmental problems requiring long-term medical support and socioeconomical services. To assess potential associations between changes in practice and survival/neurodevelopmental outcome, we performed the present study in all infants born at GA 22–24 weeks and treated at a single tertiary center from 2000 to 2009. The favorable limits of viability and neurodevelopmental outcome are discussed with special reference to the prenatal and postnatal management.

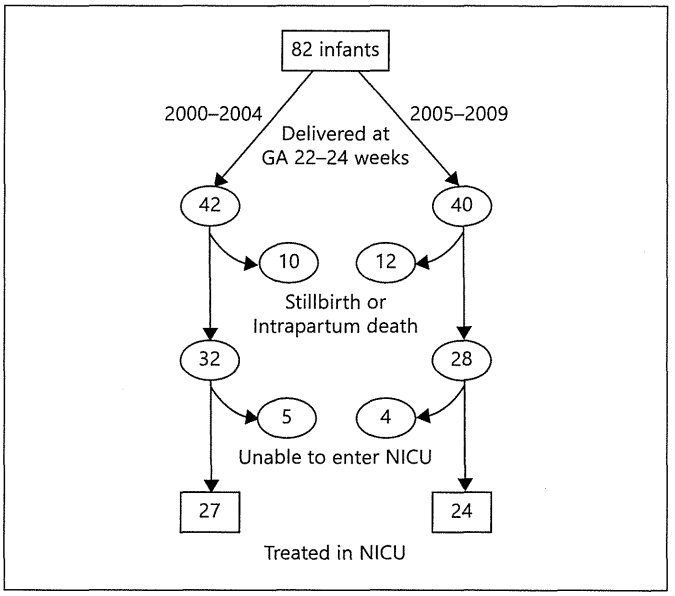

Fig. 1. Demographic characteristics of infants born at 22–24 weeks of GA delivered in 2000–2009 in our single institution. During the 10-year study period, 82 infants were delivered at GA 22–24 weeks, including 42 in 2000–2004 and 40 in 2005–2009. Of the 42 and 40 infants, 10 and 12 were stillbirths or intrapartum deaths, and the 32 and 28 were delivered as live-born infants. Of the 32 and 28 live-born infants, 5 and 4 were unable to enter the NICU because of severe asphyxia or extreme prematurity, and 27 and 24 were treated in the NICU.

Materials and Methods

Study Subjects

The study population included all infants delivered at GA 22–24 weeks at the Kyushu University Hospital in Japan from January 1st 2000 to December 31st 2009 (fig. 1). The maternal and neonatal records of all infants were studied retrospectively. The information collected included previous obstetric history, the present pregnancy and delivery, infant morbidity, treatment, survival, and neurodevelopmental outcome up to 3 years of age. A total of 51 alive infants, all free from congenital diseases, reached the NICU for intensive treatment.

Perinatal period was defined as comprising late pregnancy from GA 22 weeks until birth, labor and delivery, and the first week of life in accordance with the recommendations of the World Health Organization (WHO). Live birth and perinatal mortality were also defined by the WHO recommendations (http://www.who.int/whr/2005/en/index.html). Perinatal mortality included stillbirths and early neonatal deaths. Stillbirth was defined as fetal death before onset of labor. Intrapartum death was defined as stillbirth when the fetus was alive at the start of labor. Early neonatal death refers to a death of a live-born infant within the first 7 days of life, while death covers the remaining period up to the first year of life. GA was determined as the best obstetric estimate based on the last menstrual period, standard obstetric parameters, and ultrasonographic findings. Iatrogenic delivery represented a delivery medically or surgically induced due to maternal and/or fetal indications [8]. Antenatal steroid therapy was defined as the administration of any corticosteroid to the mother between GA 22 and 34 weeks for accelerating fetal lung maturation [9]. Surfactant administration included at least 1 dose of surfactant. Indomethacin treatment was conducted for closure of a patent ductus arteriosus (PDA) diagnosed critically or by echocardiography. Infants with body weight below the 10 percentile of the mean of the Japanese birth size standard data were classified as small for GA (SGA) [10].

Follow-up evaluations, including interval health history, neurologic evaluations, and developmental assessments (developmental quotient, DQ), were performed at 3 years of age. Developmental testing was performed using the Kyoto Scale of Psychological Development 2001 (KSPD) by trained testers. KSPD is a Japanese standard developmental test and is used to assess disabled children by most of public health centers [11]. It is an individualized face-to-face test administered by experienced psychologists to assess child's development in the following three areas: postural-motor (fine and gross motor functions); cognitive-adaptive (non-verbal reasoning or visuospatial perceptions assessed using materials such as blocks, miniature cars, and marbles), and language-social (interpersonal relationship, socializations and verbal abilities). DQ was calculated by dividing the developmental age by chronological

Table 1. Perinatal characteristics and interventions for 60 live-born infants at GA 22–24 weeks

	2000–2004 (n = 32)	2005–2009 (n = 28)	p value
Obstetric characteristics			
CAM or p-PROM	16 (50)	17 (61)	0.28
Preeclampsia	2 (6)	6 (21)	0.09
Interventions			
Iatrogenic preterm delivery	8 (25)	8 (29)	0.49
Tocolytic treatment	30 (94)	15 (54)	<0.01
Antenatal steroid	2 (6)	9 (32)	0.01
Cesarean section	12 (38)	15 (54)	0.16
Neonatal interventions			
Intubation at birth	25 (78)	24 (86)	0.34
Surfactant administration	19 (59)	20 (71)	0.24

Figures in parentheses indicate percentages. CAM = Chorioamnionitis; p-PROM = preterm-premature rupture of membrane. Iatrogenic delivery means delivery was induced by maternal and/or fetal indications. Antenatal steroid therapy was defined as administration of any corticosteroid to the mothers between GA 22 and 34 weeks for accelerating fetal lung maturation.

Table 2. Neonatal characteristics and interventions of survivors born at 22–24 weeks of GA over one year

	2000–2004 (n = 14)	2005–2009 (n = 19)	p value
Neonatal characteristics			
Male sex	8 (57)	9 (47)	0.84
Multiple birth	1 (7)	2 (11)	0.74
1-min Apgar score <4	8 (57)	16 (84)	0.18
5-min Apgar score <4	3 (21)	8 (42)	0.38
SGA	0 (0)	6 (32)	0.06
GA <24 weeks	6 (43)	7 (37)	0.50
Birthweight <400 g	0 (0)	2 (11)	0.32
Interventions			
High-frequency oscillation	10 (71)	19 (100)	0.05
Indomethacin	7 (50)	17 (89)	0.03
Ligation	3 (21)	6 (32)	0.80
Early parenteral nutrition	5 (36)	18 (95)	<0.01
Transfusion	13 (93)	19 (100)	0.88

Figures in parentheses indicate percentages. Infants with body weight below the 10 percentile of the mean of the Japanese birth size standard data were classified as SGA. Indomethacin treatment was performed for the closure of PDA diagnosed clinically or by echocardiography.

age and then multiplying the quotient by 100. The mean and one standard deviation of DQ was 100.6 and 13.4, respectively. According to the protocol Japanese Society for Follow-up Study of High-Risk Infants, we defined as a normal or borderline developmental status a DQ score over 70, a mild status as a DQ from 50 to 70, and a moderate to severe status as a DQ less than 50 [12]. The study was approved by the Institutional Review Boards of Kyushu University.

Statistics

Differences between groups were tested for significance by the χ^2 test. Multivariate logistic regression analysis was conducted for survival over one year and normal to mild neurodevelopmental delay (DQ >50) as independent variables; dependent variables included perinatal characteristics, interventions and morbidities. Only dependent variables with a p value <0.25 on univariate analysis were entered into the multiple logistic models. The statistical analyses were conducted using Excel statistics (SSRI, Japan) for Windows and SPSS software (v19; SPSS, Chicago, Ill., USA). Results with p values <0.05 were considered significant.

Results

Survival of Infants Born at 22–24 Weeks of GA between 2000–2004 and 2005–2009

During the 10-year study period, a total of 82 infants were delivered at GA 22–24 weeks, including 42 in 2000–2004 and 40 in 2005–2009 (fig. 1). Ten and 12 of them were stillbirths or intrapartum deaths, and 32 and 28 were delivered as live-born infants in 2000–2004 and 2005–2009, respectively. In 2000–2004, 18 (56%) infants died within 365 days of life including 15 early (0–6 days) and 3 late (7–27 days) neonatal deaths, and 14 (44%) survived over one year. In 2005–2009, 9 (32%) infants died, including 7 early and 1 late neonatal death, and 19 (68%) survived to 1 year. This difference in survival rate is statistically significant (p = 0.04). When perinatal characteristics and interventions were compared, the 32 live-born infants in the second period underwent less frequently maternal tocolysis (54 vs. 94%, p < 0.01) and more frequently antenatal steroid therapy (32 vs. 6%, p = 0.01) than 28 born in the first period (table 1). No other profile differed significantly between the two groups (table 2).

Survival Factors for Infants Born at 22–24 Weeks of GA

When neonatal characteristics and interventions were compared between the 14 (in 2000–2004) and 19 (in 2005–2009) survivors, the post-2005 survivors received more frequently indomethacin therapy (89 vs. 50%, p = 0.03) and early parenteral nutrition (95 vs. 36%, p < 0.01) than the pre-2004 ones (table 2).

Table 3. Clinical variables associated with a DQ >50 at 3 years of age

Variable	Infants born at 22–24 weeks of GA treated in NICU (n = 48[1])					
	univariate			multivariate		
	OR	95% CI	p value	OR	95% CI	p value
GA <24 weeks	0.19	0.05–0.67	0.02	0.14	0.03–0.67	0.01
Parenteral nutrition	4.82	1.38–16.76	0.02	1.01	0.09–10.78	0.99
Ligation	7.88	1.42–43.66	0.03	0.19	0.01–2.39	0.20
Transfusion	9.47	1.10–81.73	0.05	8.87	0.97–81.37	0.05
High-frequency oscillation	5.19	1.00–26.95	0.08	5.24	0.45–61.75	0.19
Indomethacin	2.43	0.74–7.98	0.24	9.75	0.67–141.9	0.10
1-min Apgar score <4	0.45	0.12–1.63	0.37			
Male sex	0.59	0.18–1.90	0.56			
Birthweight <400 g	3.29	0.28–39.16	0.70			
Iatrogenic preterm delivery	1.21	0.34–4.29	0.77			
5-min Apgar score <4	0.68	0.19–2.43	0.78			
Multiple birth	0.56	0.10–3.26	0.82			
SGA	1.17	0.23–5.94	0.85			
Cesarean section	1.11	0.35–3.54	0.86			
Tocolytic treatment	0.89	0.24–3.37	0.86			
Antenatal steroid	1.37	0.35–5.34	0.92			

OR = Odds ratio; CI = confidence interval. Logistic regression analysis was used to investigate the independent variables on a DQ >50. Obstetric characteristics and interventions, neonatal characteristics and interventions with a p value <0.25 on univariate analysis were entered into the multivariate logistic models.

[1] Three patients in whom neurodevelopmental status was not evaluated were excluded.

Neurological Morbidity of Survivors Born at 22–24 Weeks of GA at 3 Years of Age

Three patients (1 in the first and 2 in the second period) were not evaluated because of moving or being treated for malignancy. Seven (54%) of 13 evaluable survivors attained a normal or borderline developmental status (DQ >70) in 2000–2004, and 7 (41%) of 17 survivors obtained that level in 2005–2009. Four (31%) infants in the pre-2004 group and 7 (41%) in the post-2005 group had a moderate or severe developmental delay (DQ <50). The proportion of infants who attained a DQ >50 did not reach statistical significance in the first and the second study period (69 vs. 59%, p = 0.84).

Neurodevelopmental Factors for Attaining a DQ >50 at 3 Years of Age

The attainment of a DQ >50 in survivors at 3 years of age was negatively associated with GA <24 weeks (p = 0.02), and positively associated with ductus ligation (p = 0.02) and parenteral nutrition (p = 0.03) when assessed by univariate analysis. Multivariate analysis indicated a significant association only with GA <24 weeks (p = 0.01; table 3).

Discussion

The survival rate of infants born at GA 22–24 weeks increased significantly from 52 to 79% in a tertiary center during the decade studied. In addition, the percentage of SGA increased from 0 to 32% between the two periods. The improved survival might be due to the prenatal management including the restraint of tocolytic treatment and the more extensive use of antenatal steroid therapy, as well as to the neonatal management such as the promotion of indomethacin treatment and parenteral nutrition. However, at 3 years of age survivors born in 2005–2009 did not attain a more favorable neurodevelopment than those born in 2000–2004. The premature birth at GA <24 weeks was the most critical factor influencing neurodevelopment in survivors.

Antenatal steroid therapy has been reported to decrease the mortality of infants with GA 22–25 weeks [7, 13]. Prophylactic indomethacin may have short-term benefits for preterm infants including a reduction in the incidence of symptomatic PDA, PDA surgical ligation, and severe IVH [14]. From 2006, we routinely introduced indomethacin prophylaxis for preterm infants born at

<25 weeks of GA to reduce the risk of intraventricular hemorrhage. However, the timing of administration varied with the clinical condition of patients or individual physician preference. The nutritional problems of preterm infants have become particularly relevant to survival from NICU, as numerous studies have underlined the importance of parenteral nutrition for short- and long-term neurodevelopmental outcomes. The post-2005 survivors received more high-frequency oscillation therapy (71 vs. 100%, p = 0.05) than the pre-2004 ones. However, it is controversial to what extent indomethacin, parenteral nutrition and high-frequency oscillation could affect the mortality of these infants [15].

In the present study, although the survival of preterm infants at the limit of viability increased significantly over a decade, the neurodevelopment of the survivors (DQ >50), did not improve, and actually it deteriorated from 69 to 59%. However, since the total number of survivors who attained a borderline or normal development (DQ >70) was small, this trend did not reach statistical significance or was it possible to evaluate it with a multivariate analysis. We did not have enough infants in our single institute to evaluate survival and neurodevelopmental outcome at GA 22, 23 and 24 weeks. There are a few reports on the neurological outcome of survivors at GA 22 weeks [6, 16]. The cohort study of the Neonatal Research Network, Japan, revealed that the proportion of unimpaired or minimally impaired was 12.0% at GA 22 weeks and 20.0% at GA 23 weeks [17]. Infants born at GA 22–25 weeks are fragile and vulnerable to medical interventions because of the extreme immaturity of organ systems. If the survival rate increases and the neurodevelopmental impairment remains the same, the absolute number of infants with neurological problems will increase. However, the guideline for resuscitation of preterm infants at the limit of viability is still used in Japan. Based on the presented data, the probability of not only survival but also neurodevelopmental outcome of these infants is vital for counseling parents, informing care, and planning service. Recently, a prospective follow-up study of very low-birthweight infants in Japan has revealed that periventricular leukomalacia, gastrointestinal perforation, intraventricular hemorrhage, and moderate or severe bronchopulmonary dysplasia correlated with the developmental delay at 3 years of age [12]. Brain development occurs actively during the second and third trimesters of fetal life, with neurogenesis, neural migration, maturation, apoptosis, and synaptogenesis [18, 19]. Repeated courses of antenatal steroids have a promoting effect on the myelination in developing nonhuman primate brain [20]. Further studies are required to explore the significant association of antenatal steroids with long-term neurodevelopmental outcome in the light of their possible neuroprotective effects.

Acknowledgements

This study was supported in part by a grant from the Kyushu University Clinical Research Network Project, and the Japan Ministry of Education (No. 24791113). We thank Dr. Hideki Nakayama and Dr. Shunji Hikino for their involvement in the management of the preterm infants.

References

1 Hakansson S, Farooqi A, Holmgren PA, Serenius F, Hogberg U: Proactive management promotes outcome in extremely preterm infants: a population-based comparison of two perinatal management strategies. Pediatrics 2004;114:58–64.
2 Hintz SR, Kendrick DE, Vohr BR, Poole WK, Higgins RD, Neo NICHHD: Changes in neurodevelopmental outcomes at 18 to 22 months' corrected age among infants of less than 25 weeks' gestational age born in 1993–1999. Pediatrics 2005;115:1645–1651.
3 Hoekstra RE, Ferrara TB, Couser RJ, Payne NR, Connett JE: Survival and long-term neurodevelopmental outcome of extremely premature infants born at 23–26 weeks' gestational age at a tertiary center. Pediatrics 2004; 113:e1–e6.
4 Markestad T, Kaaresen PI, Ronnestad A, Reigstad H, Lossius K, Medbo S, Zanussi G, Engelund IE, Skjaerven R, Irgens LM: Early death, morbidity, and need of treatment among extremely premature infants. Pediatrics 2005;115:1289–1298.
5 Fellman V, Hellstrom-Westas L, Norman M, Westgren M, Kallen K, Lagercrantz H, Marsal K, Serenius F, Wennergren M: One-year survival of extremely preterm infants after active perinatal care in Sweden. JAMA 2009;301: 2225–2233.
6 Itabashi K, Horiuchi T, Kusuda S, Kabe K, Itani Y, Nakamura T, Fujimura M, Matsuo M: Mortality rates for extremely low birth weight infants born in Japan in 2005. Pediatrics 2009; 123:445–450.
7 Mori R, Kusuda S, Fujimura M: Antenatal corticosteroids promote survival of extremely preterm infants born at 22 to 23 weeks of gestation. J Pediatr 2011;159:110–114.e111.
8 Goldenberg RL, Culhane JF, Iams JD, Romero R: Epidemiology and causes of preterm birth. Lancet 2008;371:75–84.
9 Roberts D, Dalziel S: Antenatal corticosteroids for accelerating fetal lung maturation for women at risk of preterm birth. Cochrane Database Syst Rev 2006;■■:CD004454.
10 Yoshida SH, Unno N, Kagawa H, Shinozuka N, Kozuma S, Taketani Y: Sonographic determination of fetal size from 20 weeks of gestation onward correlates with birth weight. J Obstet Gynaecol Res 2001;27:205–211.
11 Tamaru S, Kikuchi A, Takagi K, Wakamatsu M, Ono K, Horikoshi T, Kihara H, Nakamura T: Neurodevelopmental outcomes of very low birth weight and extremely low birth weight infants at 18 months of corrected age associated with prenatal risk factors. Early Hum Dev 2011;87:55–59.

12 Kono Y, Mishina J, Yonemoto N, Kusuda S, Fujimura M: Neonatal correlates of adverse outcomes in very low-birthweight infants in the NICU network. Pediatr Int 2011;53:930–935.
13 Carlo WA, McDonald SA, Fanaroff AA, Vohr BR, Stoll BJ, Ehrenkranz RA, Andrews WW, Wallace D, Das A, Bell EF, Walsh MC, Laptook AR, Shankaran S, Poindexter BB, Hale EC, Newman NS, Davis AS, Schibler K, Kennedy KA, Sanchez PJ, Van Meurs KP, Goldberg RN, Watterberg KL, Faix RG, Frantz ID 3rd, Higgins RD: Association of antenatal corticosteroids with mortality and neurodevelopmental outcomes among infants born at 22 to 25 weeks' gestation. JAMA 2011;306:2348–2358.
14 Fowlie PW, Davis PG, McGuire W: Prophylactic intravenous indomethacin for preventing mortality and morbidity in preterm infants. Cochrane Database Syst Rev 2010;■■:CD000174.
15 Morgan J, Young L, McGuire W: Delayed introduction of progressive enteral feeds to prevent necrotising enterocolitis in very low birth weight infants. Cochrane Database Syst Rev 2011;■■:CD001970.
16 Sugiura T, Kouwaki M, Togawa Y, Sugimoto M, Togawa T, Koyama N: Neurodevelopmental outcomes at 18 months' corrected age of infants born at 22 weeks of gestation. Neonatology 2011;100:228–232.
17 Ishii N, Kono Y, Yonemoto N, Kusuda S, Fujimura M: Outcomes of infants born at 22 and 23 weeks' gestation. Pediatrics 2013;132:62–71.
18 Huttenlocher PR: Morphometric study of human cerebral cortex development. Neuropsychologia 1990;28:517–527.
19 Huttenlocher PR, Dabholkar AS: Regional differences in synaptogenesis in human cerebral cortex. J Comp Neurol 1997;387:167–178.
20 Shields A, Thomson M, Winter V, Coalson J, Rees S: Repeated courses of antenatal corticosteroids have adverse effects on aspects of brain development in naturally delivered baboon infants. Pediatr Res 2012;71:661–667.

9. Gong YY, Xie L, Zhou WP et al. Glucose and lipid profile of a long-lived rural Han Chinese population and their families in southwest China. J Am Geriatr Soc 2009;57:567–568.
10. Ye JJ, Li JC, Peng L et al. Nonagenarians and centenarians in a rural Han Chinese population: Lifestyle and epidemics. J Am Geriatr Soc 2009; 57:1723–1724.

Case Reports

ENDOCRINE AND METABOLIC ABNORMALITIES IN A GIRL WITH CHILDHOOD WERNER SYNDROME: CASE REPORT

To the Editor: Werner syndrome (WS) is a rare progeroid syndrome of autosomal-recessive inheritance that German ophthalmologist Otto Werner first reported in 1904. The frequency of WS is as high as 1 in 40,000 in Japan, with consanguineous marriage noted in approximately 40% of cases, although no regional localization of cases has been recognized.[1,2] Most progeroid phenotypes are clinically typical, including the graying and loss of hair; hoarseness and scleroderma-like skin changes emerging in the 20s; and juvenile cataracts, insulin-resistant diabetes mellitus, hypogonadism, ulceration of the skin, osteoporosis, and soft tissue calcification arising in the 30s. The most severe and lethal conditions are malignant tumors and cardiovascular or cerebrovascular diseases resulting from premature atherosclerosis in the 40s and 50s.[1–4] Mean age at diagnosis was 36.7 in individuals who presented with typical signs of WS.[3] In contrast, individuals who develop the disease in childhood are not usually reported primarily because of the variety of nonspecific symptoms and lack of cardinal signs during the teenage years. The case of a girl diagnosed with WS at 17 is herein reported.

The girl's parents were second cousins without a family history suggesting the presence of genetic diseases, including progeroid syndromes. The girl was healthy at birth and exhibited normal growth and development in infancy. Starting at 6 years old, she gradually developed facial erythema (Figure 1) and failure to grow. At 10 years old, her parents consulted a pediatrician regarding her growth failure and chronic fatigue of unknown etiology. Clinical and laboratory examinations identified a diagnosis of hypothyroidism, and levothyroxine treatment was started, but she discontinued the medication after several months. At 17 years old, she again consulted a physician and was referred to the hospital for systematic evaluation.

She was 141 cm (3.3 standard deviations below the mean) tall and weighed 33.2 kg (2.7 standard deviations below the mean), and her body mass index was 16.7 kg/m^2. She had slightly gray hair, erythema on both cheeks, and dry skin over her entire body. Laboratory findings demonstrated hepatic dysfunction (aspartate aminotransferase, 132 U/L (normal range (NR) 13–33 U/L); alanine aminotransferase, 252 U/L (NR 6–30 U/L); gamma-glutamyl transpeptidase, 51 U/L (NR 10–47 U/L)) and dyslipidemia (triglycerides, 221 mg/dL (NR, 30–149 mg/dL); low-density lipoprotein cholesterol, 140 mg/dL (NR <139)), with normal serum creatine phosphokinase, blood urea nitrogen, and creatinine levels. Metabolic and endocrinological studies revealed hypothyroidism (basal thyroid-stimulating hormone (TSH), 11.22 μU/mL (NR 0.27–4.20 μU/mL); free thyroxine, 0.82 ng/dL (NR 1.00–1.80 ng/dL)) with a remarkably high TSH level after a thyrotropin releasing hormone loading test (58.48 μU/mL at 60 minutes (NR 10–25 μU/mL)). An oral glucose tolerance test with 75-g oral glucose loading showed borderline glucose intolerance with remarkable insulin resistance (blood glucose, 197 mg/dL (NR 60–125 mg/dL); insulin, 563 μU/mL at 120 minutes (NR <300)). Ultrasonography demonstrated an atrophic thyroid and marked fatty liver. Brachial–ankle pulse wave velocity indicated slight arteriosclerotic changes (right 1,188 cm/s, left 1,157 cm/s, mean 952 ± 103 cm/s). Bilateral ovary hypoplasia and a right ovarian cyst were detected on magnetic resonance imaging. Ophthalmological study revealed bilateral cataracts. There were no signs of osteoporosis of the lumbar spine (bone mineral density 0.968 g/cm^3; Z-score −0.4). No calcification of the Achilles tendon, a cardinal sign of WS in adulthood,[1] was detected on X-ray examination. Genetic tests identified a homozygous mutation of IVS25–1G>C in the *WRN* gene, one of the most common mutations in Japanese individuals with WS. Medical treatment with levothyroxine sodium hydrate at a dose of 100 μg/d quickly normalized the girl's thyroid function, with an associated increase in her vigor. Subsequent biguanide therapy (750 mg/d) was discontinued within 1 week because of abdominal pain.

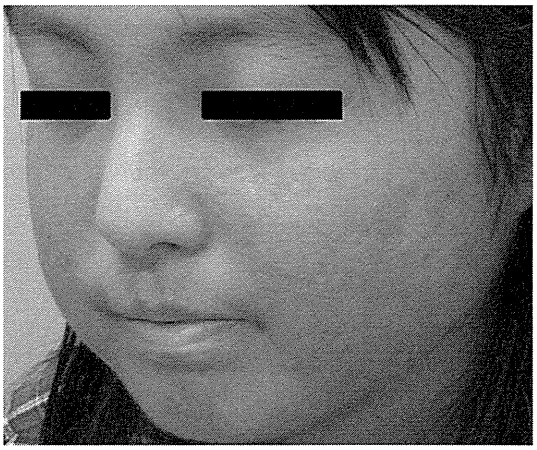

Figure 1. Facial erythema and beak-like appearance.

Based on the clinical features reported in previous studies, the characteristic abnormalities in metabolism observed in individuals with WS are mainly attributed to peripheral lipoatrophy with insulin insensitivity or dyslipidemia.[5] Endocrinological problems in the setting of WS primarily derive from the impaired secretion of hormones due to premature aging of endocrine organs, and empirically, hypogonadism, hypothyroidism, and hypopituitarism are the major endocrinological concerns in individuals with WS. Although these conditions may be present in childhood, no clinical studies have reported such features, probably because of the difficulty in diagnosing WS in individuals with nonspecific symptoms. The present case therefore provides important and valuable information. First, hypothyroidism of atrophic thyroid glands in addition to pituitary and hypothalamic dysfunction can appear as early as 10 years of age. Second, marked insulin insensitivity due to a lipodystrophic phenotype can arise in

adolescence. Third, the subject gradually exhibited hypergonadotrophic hypogonadism in her teens. Hence, nonspecific metabolic and endocrinological conditions, as well as atrophic skin, growth failure, and bilateral cataracts, may be characteristic findings of WS in childhood. According to previous reports,[2] an earlier onset of clinical symptoms is associated with a shorter life span. Hence, it is critically important to make a proper diagnose at an early age to initiate careful and consistent observation and provide early therapeutic intervention.

Naoko Toda, MD
Kenji Ihara, MD, PhD
Department of Pediatrics, Graduate School of Medical Sciences, Kyushu University, Fukuoka, Japan

Minoru Takemoto, MD, PhD
Koutaro Yokote, MD, PhD
Department of Clinical Cell Biology and Medicine Graduate School of Medicine, Chiba University, Chiba Japan

Toshiro Hara, MD, PhD
Department of Pediatrics, Graduate School of Medical Sciences, Kyushu University, Fukuoka, Japan

ACKNOWLEDGMENTS

Conflict of Interest: The editor-in-chief has reviewed the conflict of interest checklist provided by the authors and has determined that the authors have no financial or any other personal conflicts with respect to this work.

Author Contributions: Study concept and design: Toda, Ihara. Acquisition of subject and data: Toda, Ihara. Study design and interpretation of the data: Watanabe, Takemoto, Yokote. Preparation of manuscript: Toda, Ihara.

Sponsor's Role: No sponsors.

REFERENCES

1. Takemoto M, Mori S, Kuzuya M et al. Diagnostic criteria for Werner syndrome based on Japanese nationwide epidemiological survey. Geriatr Gerontol Int 2013;13:475–481.
2. Goto M, Ishikawa Y, Sugimoto M et al. Werner syndrome: A changing pattern of clinical manifestations in Japan (1917–2008). Biosci Trends 2013;7:13–22.
3. Goto M. Hierarchical deterioration of body systems in Werner's syndrome: Implications for normal ageing. Mech Ageing Dev 1997;98:239–254.
4. Lauper JM, Krause A, Vaughan TL et al. Spectrum and risk of neoplasia in Werner syndrome: A systematic review. PLoS ONE 2013;8:e59709.
5. Donadille B, D'Anella P, Auclair M et al. Partial lipodystrophy with severe insulin resistance and adult progeria Werner syndrome. Orphanet J Rare Dis 2013;8:106.

ONCE-WEEKLY TOLVAPTAN FOR CHRONIC SYMPTOMATIC HYPONATREMIA DUE TO SYNDROME OF INAPPROPRIATE SECRETION OF ANTI-DIURETIC HORMONE

To the Editor: An 83-year-old man was diagnosed with syndrome of inappropriate secretion of anti-diuretic hormone (SIADH) in 2009, when he developed severe symptomatic hyponatremia (sodium 119 mmol/L) after a respiratory tract infection. He was taking levothyroxine for hypothyroidism. He was unable to tolerate demeclocycline because he had hepatitis, and since then, his sodium had been maintained at approximately 125 mmol/L with fluid restriction. In December 2011, he fell and fractured his hip. At that time, his sodium was 123 mmol/L. He had a hemiarthroplasty and was hospitalized for 6 weeks.

In February 2012, he was admitted after a seizure. Laboratory tests showed sodium 118 mmol/L, urea 5.2 mmol/L, and creatinine 62 μmol/L. Despite strict fluid restriction, his sodium did not improve, and he remained confused and disoriented. He was started on tolvaptan 15 mg on alternate days to avoid rapid correction. He had profuse diuresis, and by Day 4 (just after two doses), his sodium had increased to 133 mmol/L and his urea from 5 to 16 mmol/L, and his symptoms had improved dramatically.

To avoid overcorrection and renal failure, tolvaptan was stopped, and fluid restriction was restarted, but his sodium fell to 119 mmol/L, and his symptoms returned within 2 days, so it was decided to try tolvaptan once a week. To avoid wide fluctuations in his sodium, he was advised to drink until thirst is eliminated for 4 days after taking tolvaptan and to restrict his fluids 3 days before the next dose. His sodium increased by 2 to 3 mmol/L per day for 3 days after tolvaptan and fell by 1 to 2 mmol/L per day after Day 3, and he remained symptom free.

After discharge, he took tolvaptan 15 mg once a week for 12 months and then 15 mg every 6 days because of tiredness and lethargy returning 5 days after taking tolvaptan. During this period, his sodium fluctuated around 125 mmol/L (range 122–133 mmol/L; Figure 1). Despite the fluctuation in his sodium, he remained asymptomatic and had not been admitted to the hospital. In February 2014, he was admitted with sepsis and died of multiorgan failure nearly 2 years after taking tolvaptan.

Hyponatremia is the most frequent electrolyte imbalance in elderly adults, and severe hyponatremia (sodium < 125 mmol/L) is found in up to 6% of hospitalized older adults.[1] Hyponatremia due to SIADH is often chronic and asymptomatic, but sodium levels of less than 125 mmol/L can cause unsteadiness, falls, attention deficit, and fractures in elderly adults.[2,3] Even though fluid restriction is effective, it is difficult to sustain over the long term.

Tolvaptan is a vasopressin receptor antagonist and is effective in the treatment of hyponatremia due to SIADH by promoting free water excretion.[4–6] Adverse effects include thirst, dehydration, and too-rapid correction of sodium (which can lead to complications). In clinical trials, 7% of participants had an increase in serum sodium of 8 mmol/L at 8 hours, and 2% had an increase of more than 12 mmol/L at 24 hours.[6]

The major constraints in using this drug are its cost, rapid correction with the risk of osmotic demyelination syndrome, rebound hyponatremia after stopping the drug, and uncertainty regarding long-term use.

Concerns have also been raised in using this drug over the long term because it could cause liver injury, and the Food and Drug Administration has warned that tolvaptan

OPEN ACCESS Freely available online

PLOS | ONE

Reprogramming Suppresses Premature Senescence Phenotypes of Werner Syndrome Cells and Maintains Chromosomal Stability over Long-Term Culture

Akira Shimamoto[1]*, Harunobu Kagawa[1], Kazumasa Zensho[1], Yukihiro Sera[1], Yasuhiro Kazuki[2], Mitsuhiko Osaki[2,3], Mitsuo Oshimura[2], Yasuhito Ishigaki[4], Kanya Hamasaki[5], Yoshiaki Kodama[5], Shinsuke Yuasa[6], Keiichi Fukuda[6], Kyotaro Hirashima[7], Hiroyuki Seimiya[7], Hirofumi Koyama[8], Takahiko Shimizu[8], Minoru Takemoto[9], Koutaro Yokote[9], Makoto Goto[10], Hidetoshi Tahara[1]*

1 Department of Cellular and Molecular Biology, Graduate School of Biomedical & Health Sciences, Hiroshima University, Hiroshima, Japan, **2** Department of Biomedical Science, Institute of Regenerative Medicine and Biofunction, Graduate School of Medical Science, Tottori University, Yonago, Japan, **3** Division of Pathological Biochemistry, Faculty of Medicine, Tottori University, Yonago, Japan, **4** Medical Research Institute, Kanazawa Medical University, Kahoku, Ishikawa, Japan, **5** Department of Genetics, Radiation Effects Research Foundation, Hiroshima, Japan, **6** Department of Cardiology, Keio University School of Medicine, Tokyo, Japan, **7** Division of Molecular Biotherapy, The Cancer Chemotherapy Center, Japanese Foundation For Cancer Research, Tokyo, Japan, **8** Department of Advanced Aging Medicine, Chiba University Graduate School of Medicine, Chiba, Japan, **9** Department of Clinical Cell Biology and Medicine, Chiba University Graduate School of Medicine, Chiba, Japan, **10** Division of Orthopedic Surgery & Rheumatology, Tokyo Women's Medical University Medical Center East, Tokyo, Japan

Abstract

Werner syndrome (WS) is a premature aging disorder characterized by chromosomal instability and cancer predisposition. Mutations in *WRN* are responsible for the disease and cause telomere dysfunction, resulting in accelerated aging. Recent studies have revealed that cells from WS patients can be successfully reprogrammed into induced pluripotent stem cells (iPSCs). In the present study, we describe the effects of long-term culture on WS iPSCs, which acquired and maintained infinite proliferative potential for self-renewal over 2 years. After long-term cultures, WS iPSCs exhibited stable undifferentiated states and differentiation capacity, and premature upregulation of senescence-associated genes in WS cells was completely suppressed in WS iPSCs despite *WRN* deficiency. WS iPSCs also showed recapitulation of the phenotypes during differentiation. Furthermore, karyotype analysis indicated that WS iPSCs were stable, and half of the descendant clones had chromosomal profiles that were similar to those of parental cells. These unexpected properties might be achieved by induced expression of endogenous telomerase gene during reprogramming, which trigger telomerase reactivation leading to suppression of both replicative senescence and telomere dysfunction in WS cells. These findings demonstrated that reprogramming suppressed premature senescence phenotypes in WS cells and WS iPSCs could lead to chromosomal stability over the long term. WS iPSCs will provide opportunities to identify affected lineages in WS and to develop a new strategy for the treatment of WS.

Citation: Shimamoto A, Kagawa H, Zensho K, Sera Y, Kazuki Y, et al. (2014) Reprogramming Suppresses Premature Senescence Phenotypes of Werner Syndrome Cells and Maintains Chromosomal Stability over Long-Term Culture. PLoS ONE 9(11): e112900. doi:10.1371/journal.pone.0112900

Editor: Zhongjun Zhou, The University of Hong Kong, Hong Kong

Received August 9, 2014; **Accepted** October 16, 2014; **Published** November 12, 2014

Data Availability: The authors confirm that all data underlying the findings are fully available without restriction. The microarray dataset are available from the NCBI Gene Expression Omnibus database (accession number GSE62114).

Funding: This work was supported by a Grant-in-Aid for Challenging Exploratory Research No. 25670030 (to A.S) and for Scientific Research No. 20014015 (to H.T) and No. 24590902 (to M.G) from the Ministry of Education, Culture, Sports, Science and Technology of Japan. This work was also supported by a Health and Labor Sciences Research Grant from the Ministry of Health Labor and Welfare of Japan (to A.S). The funders had no role in study design, data collection and analysis, decision to publish, or preparation of the manuscript.

Competing Interests: The authors have declared that no competing interests exist.

* Email: shim@hiroshima-u.ac.jp (AS); toshi@hiroshima-u.ac.jp (HT)

Introduction

Werner syndrome (WS) is a rare human autosomal recessive disorder characterized by early onset of aging-associated diseases, chromosomal instability, and cancer predisposition [1,2]. Fibroblasts from WS patients exhibit premature replicative senescence [3], and *WRN*, a gene responsible for the disease, encodes a RecQ-type DNA helicase [4–7], that is involved in maintenance of chromosome integrity during DNA replication, repair, and recombination [8,9]. WRN helicase is known to interact with a variety of proteins associated with DNA metabolism including proteins of replication fork progression, base excision repair, and telomere maintenance [8,9]. The dysfunction of WRN helicase causes defects in telomeric lagging-strand synthesis and telomere loss during DNA replication [10]. Further, it is also reported that telomere loss caused by a defect in WRN helicase involves chromosome end fusions that are suppressed by telomerase [11]. These observations suggest that premature senescence in WS cells reflects defects in telomeric lagging-strand synthesis followed by accelerated telomere loss during DNA replication.

Somatic cell reprogramming follows the introduction of several pluripotency genes including Oct3/4, Sox2, Klf4, c-myc, Nanog

and Lin-28 into differentiated cells such as dermal fibroblasts, blood cells, and other cell types [12–17]. During reprogramming, somatic cell-specific genes are suppressed, and embryonic stem cell (ESC)-specific pluripotency genes are induced, leading to the generation of iPSCs with undifferentiated states and pluripotency [18]. In addition, ESC-like infinite proliferative potential is directed by induction of the endogenous telomere reverse-transcriptase catalytic subunit (hTERT) gene and the reactivation of telomerase activity during reprogramming [13,18].

Recently, Cheung et al. demonstrated that cells from WS patients were successfully reprogrammed into iPSCs with restored telomere function, suggesting that the induction of hTERT during reprogramming suppresses telomere dysfunction in WS cells lacking *WRN* [19]. However, the effects of long-term culture on the undifferentiated states, self-renewal abilities, and differentiation potentials of WS iPSCs remain unknown. In a previous study, progressive telomere shortening and loss of self-renewal ability were observed in iPSCs from dyskeratosis congenital patient cells in a long-term culture [20], warranting the evaluation of the properties of patient cell-derived iPSCs with telomere dysfunctions over the long term.

In this study, we cultured WS iPSCs with self-renewal capacity and infinite proliferative potential for over 2 years and reported similar properties to those of normal iPSCs including undifferentiated states and differentiation ability. Notably, WS iPSCs maintained stable karyotypes and their potential to recapitulate premature senescence phenotypes during differentiation over the long term. The present data demonstrate that reprogramming suppresses premature senescence phenotypes in WS cells by reversing the aging process and restoring telomere maintenance over the long term.

Materials and Methods

Cell lines

WS patients were diagnosed on the basis of clinical symptoms and *WRN* gene mutations. A0031 WS patient fibroblasts from a 37-year-old male were obtained from Goto Collection of RIKEN Bioresource Center (https://www.brc.riken.jp/lab/cell/english/index_gmc.shtml) [21], and WSCU01 patient fibroblasts were isolated from a 63-year-old Japanese male who was diagnosed at Chiba University. Both fibroblast isolates had type 4/6 heterozygous mutations. TIG-3 human fetal lung-derived fibroblast cells and WS patient-derived fibroblasts were used to generate iPSC lines. PLAT-A cells (kindly provided from Dr. Toshio Kitamura) were used to produce retroviruses [22]. SNL 76/7 (SNL) cells (DS pharma biomedical) were used as feeder layers for reprogramming of fibroblasts and maintenance of iPSCs. The human fibroblast-derived iPSC line iPS-TIG114-4f1 was obtained from the National Institute of Biomedical Innovation [23].

PLAT-A cells, TIG-3 fibroblasts, TIG-114 fibroblasts from the 36-year-old male, and SNL cells were grown in the Dulbecco's modified Eagle's medium (DMEM; Sigma) supplemented with 10% fetal bovine serum (FBS; Hyclone) and antibiotics (Invitrogen). WS fibroblasts were maintained on collagen-coated dishes (Nitta Gelatin), SNL cells were maintained on gelatin-coated dishes (Nitta Gelatin), and iPSCs were maintained in the ES medium comprising Knockout DMEM (Invitrogen) supplemented with 20% Knockout Serum Replacement (Invitrogen), glutamine, non-essential amino acids, β-mercaptoethanol and 4-ng/ml basic FGF. All cells were maintained at 37°C under 5% CO_2 atmosphere.

Generation of iPSCs

The generation of iPSCs was performed as described previously [13]. Briefly, 2×10^6 PLAT-A cells were plated in T25 flasks (Biocoat, BD Falcon), and were transfected with 4 μg pMXs-OCT3/4, SOX2, KLF-4, and c-myc (Addgene) 1 day later. Twenty-four hours after transfection, the culture medium was replaced with a fresh medium and cells were incubated for 24 h prior to harvest of viral supernatants. Viral supernatants containing Yamanaka factors were combined in even ratios.

For reprogramming experiments, 3×10^5 fibroblasts were seeded on 60-mm dishes and were infected with viral supernatants containing Yamanaka factors in the presence of 8 μg/ml polybrene 1 day later. Four days after infection, fibroblasts were harvested, and 1×10^5 cells were reseeded onto mitomycin C-inactivated SNL feeder layers on 100-mm dishes. Twenty-four hours after reseeding, the medium was replaced with the ES medium, and cultures were maintained by replacing the medium every other day. Approximately 30 days after retroviral transduction, emerging iPSC colonies with ESC colony-like flat and round shapes were picked up by mechanical dissection and were plated onto fresh feeder layers on 4-well plates (Thermo Scientific Nunc). Subsequently, iPSC lines were established by successive passages onto fresh feeder layers with split ratios between 1:3 and 1:5 using dispase (Roche Applied Science).

Alkaline phosphatase activity

Undifferentiated states of emerging colonies were examined using alkaline phosphatase staining. After formalin fixation, colonies were stained with reaction buffer containing 100 mM Tris-Cl (pH 8.5), 0.25 mg/ml Naphthol AS-BI phosphate (Sigma) and 0.25 mg/ml fast red violet LB salt (Sigma).

Embryoid body formation and in vitro differentiation

Clumps of iPSCs were transferred to non-adherent polystyrene dishes containing the ES medium without basic FGF to form embryoid bodies (EBs). The medium was replaced every other day. After 8 days of floating culture, EBs were transferred onto gelatin-coated plates and were maintained in DMEM supplemented with 10% FBS, β-mercaptoethanol, and antibiotics for another 8 days. For detection of senescence phenotypes during differentiation, Y-27632-treated iPSCs were dissociated into single cell suspensions with Accutase (Innovative Cell Technologies) and 1×10^4 cells were transferred into 96-well V-shaped bottom plates (Greiner Bio-One) to form evenly sized EBs. After 12 days of EB formation in the ES medium without basic FGF, EBs were cultured in DMEM supplemented with 10% FBS, β-mercaptoethanol, and antibiotics.

Teratoma formation

After harvest, 1×10^6 iPSCs were injected into the testes of a severe combined immunodeficient (SCID) mice (CREA, Japan). Three months after injection, tumors were dissected and were fixed using 4% paraformaldehyde. Subsequently, dissected tumor tissues were embedded in paraffin and were sliced and stained with hematoxylin and eosin.

Western blot

Whole cell lysates were prepared in SDS sample buffer and subjected to electrophoresis on 8% SDS-polyacrylamide gels, and separated proteins were transferred onto PVDF membranes (FluoroTrans W, Pall Corporation). Membranes were blocked with TBS-T containing 5% skim milk and were then incubated with anti-WRN (1:500, 4H12, Abcom) or anti-β-actin (1:30000,

Ac-15, Sigma) monoclonal antibodies for 3 h at room temperature. Membranes were then washed with TBS-T and were incubated with horseradish peroxidase-conjugated anti-mouse IgG (1:5000, NA931V, GE) for 1 h at room temperature. Chemiluminescence reactions were performed using Western Lightning Plus-ECL (PerkinElmer) and were detected using exposure of x-ray films.

Mutation analysis

The DNA fragments mut.4 (c.3139-1G>C) and mut.6 (c.1105C>T) were amplified with the primer pairs WS_mut4_U, GGTAAACGGTGTAGGAGTCTGC and WS_mut4_L, CTTGTGAGAGGCCTATAAACTGG, and WS_mut6_U, TGAAGATTCAACTACTGGGGGAGTAC and WS_ mut6_L, ACGGGAATAAAGTCTGCCAGAACC, respectively, using genomic DNA as a template. Mutations were analyzed by direct sequencing using these PCR primers.

Short tandem repeat (STR) analysis

Genomic DNAs were purified from WS fibroblasts and their derivative iPSC clones using phenol/chloroform extraction and were then used for analysis using a Cell ID System (Promega). PCR products were analyzed using an Applied Biosystems 3130xl Genetic Analyzer and GeneMapper software.

Gene expression profiling

Cy3-labeled total RNAs were hybridized onto Human Genome U133 Plus 2.0 Arrays (GeneChip, Affymetrix). Arrays were then scanned using the GeneChip Scanner 3000 7G (Affymetrix), and the obtained data were analyzed by Affymetrix Expression Console Software. The microarray dataset has been deposited in the NCBI Gene Expression Omnibus database under Series Accession GSE62114.

Measurement of telomere length

Genomic DNAs were digested using *Hinf*I restriction enzyme (TakaraBio), and were subjected to electrophoresis on 1% agarose gels. Size-fractionated DNAs were transferred onto Hybond-N+ membranes (GE). Membranes were hybridized with a digoxigenin-labeled $(CCCTAA)_4$ probe, and TRFs were detected using TeloTAGGG Telomere Length Assays (Roche Applied Science) according to the manufacturer's instructions.

RT-PCR and real-time qRT-PCR analysis of mRNA expression

Total RNA was prepared using RNeasy spin columns (Qiagen) according to the manufacturer's instructions. RT-PCR was performed with 0.1 μg of total RNA using SuperScript One-Step RT-PCR (Invitrogen). Semi-quantitative analysis was performed after converting total RNA into cDNA using a High Capacity RNA-to-cDNA kit (Life Technologies), and real-time PCR was performed using a Rotor-Gene SYBR Green PCR kit (Qiagen). Relative gene expression levels were analyzed according to the ΔΔCt method using Ct values of GAPDH mRNA as an internal control. Primer sequences are listed in Tables S1 and S2.

Immunofluorescence cytochemistry

Following fixation of iPSCs and differentiated cells with 4% paraformaldehyde for 15 min at 4°C, cells were permeabilized with 0.1% Triton X-100, washed with PBS containing 2% BSA, and incubated with primary antibodies diluted in PBS containing 2% BSA.

Primary antibodies against Nanog (1:200, Cell Signaling, D73G4), SSEA-4 (1:200, Cell Signaling, MC813), Tra-1-60 (1:200, Cell Signaling, #4746), Tra-1-81 (1:200, Cell Signaling, #4745), βIII-tubulin (1:200, Millipore, TU-20), desmin (1:200, Neomarkers, RB-9014-P0), vimentin (1:200, Santa Cruz, V9), and α-fetoprotein (1:500, Sigma, HPA010607) were detected using the secondary antibodies Alexa 488-conjugated anti-goat IgG (1:500, Invitrogen, A11055), Alexa 488-conjugated anti-mouse IgG (1:500, Invitrogen, A11001), Alexa 488-conjugated anti-mouse IgM (1:500, Invitrogen, A21042), and Alexa 488-conjugated anti-rabbit IgG (1:500, Invitrogen, A11013). Cell nuclei were stained with 1- μg/ml 4',6-diamidino-2-phenylindole (DAPI).

Karyotype analysis

After culturing iPSCs in the ES medium containing 100-ng/ml colcemid for 5 h at 37°C, cells were harvested using trypsin and were treated with 0.075 M KCl for 15 min at 37°C. Cells were then fixed in Carnoy's fluid, and chromosome slides were prepared. G-banding analysis was conducted using a previously described method [24].

M-FISH was performed with the Multi-color probe kit "24XCyte" (MetaSystems, Altlussheim, Germany) according to the manufacturer's protocol with slight modifications. Briefly, probes were denatured at 75°C for 5 min and were hybridized to metaphase spreads, which were denatured in 0.07 N NaOH at room temperature for 1 min. Slides were then incubated at 37°C for 2 nights and were then washed in 0.4× SSC at 72°C for 2 min, in 2× SSC containing 0.05% Tween 20 at room temperature for 30 s, and in 2× SSC at room temperature for 1 min, and the mounting medium (DAPI, 125 ng/ml) and a cover slip were applied. Acquisition and analysis of M-FISH images were performed using a CytoVision ChromoFluor System (Applied Imaging, Newcastle upon Tyne, UK).

Transduction of hTERT gene

PT67 retrovirus packaging cells (Takara Bio USA, Madison, WI, USA) were transfected with pMSCV-hTERT-puro using GenePorter II according to the manufacturer's protocol. After 24 h, the culture medium was replaced, cells were incubated for a further 24 h period, and viral supernatants were harvested, A0031 and WSCU01 WS fibroblasts were infected with viral supernatant in the presence of 8 μg/ml polybrene. Confluent infected cells were then split into 2 new dishes, and puromycin selection of infected cells was initiated at the following passage. Confluent infected cells were then passaged in 4-fold dilutions, leading to an increase in 2 population doubling levels for each passage.

SA-β-gal assay

SA-β-gal staining was performed as described by Debacq-Chainiaux et al. [25].

Ethical statement

This study was approved by the Ethics Review Board of the Graduate School of Medicine, Chiba University and was conducted in accordance with the Declaration of Helsinki. Written informed consents were obtained from patients prior to tissue harvesting and iPSC generation, and patients were entitled to the protection of confidential information. Genome/gene analyses performed in this study were approved by the Ethics Committee for Human Genome/Gene Analysis Research at Hiroshima University. All animal experiments were performed in strict compliance with the protocol approved by the Institutional Animal Care and Use Committee of Tottori University (13-Y-

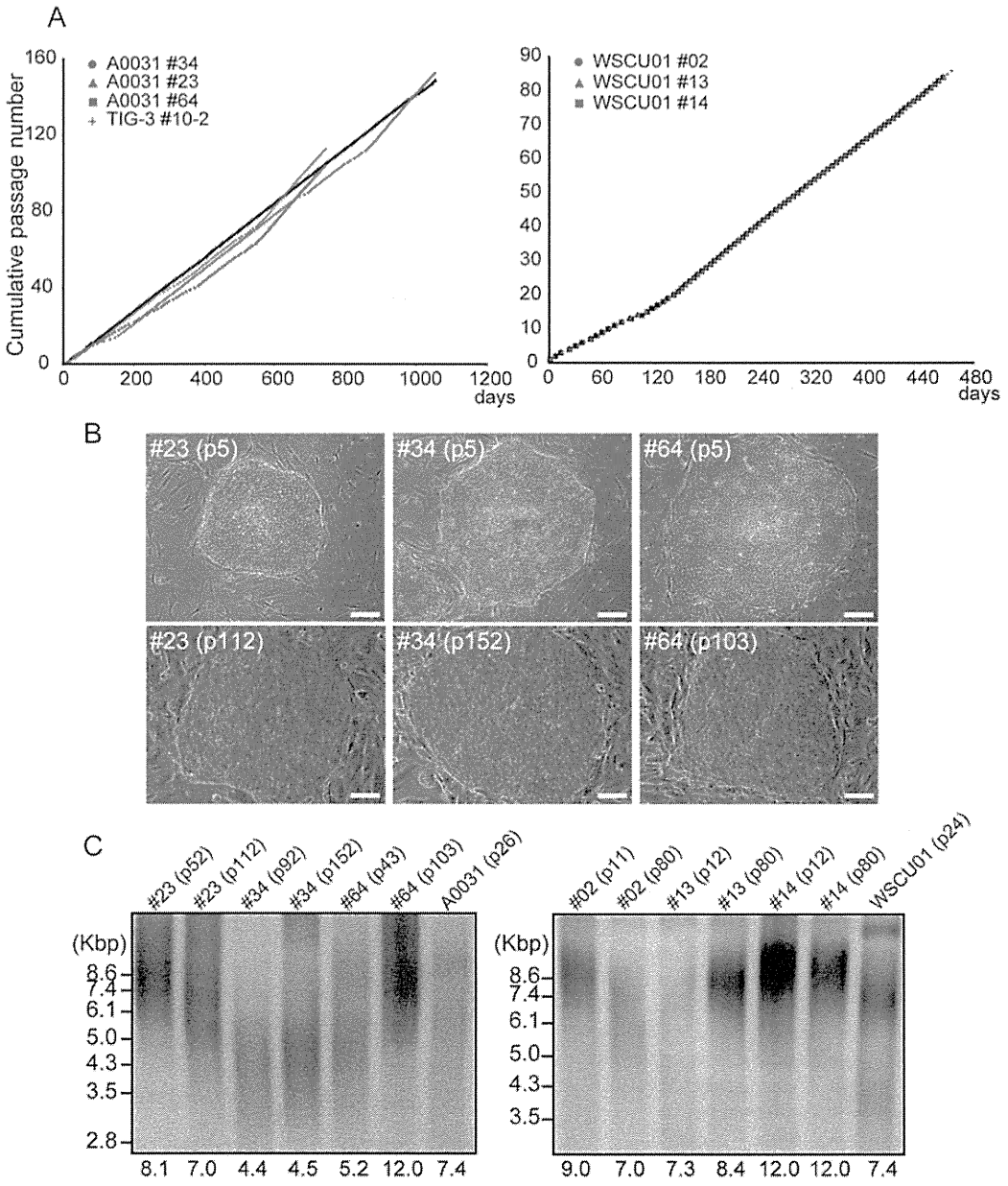

Figure 1. Infinite Proliferation of WS iPSCs after Long-Term Culture. (A) Cumulative passage number for WS iPSCs. (B) Colony morphologies of A0031-derived WS iPSC clones in early and late passages. Bars = 100 μm. (C) TRF length analysis of WS iPSC clones in early and late passages.
doi:10.1371/journal.pone.0112900.g001

18), and the Animal Care and Use Committee of Chiba University (25–131). All recombinant DNA experiments were performed in strict conformance with the guidelines of the Institutional Recombinant DNA Experiment Safety Committee at Hiroshima University.

Results

Infinite proliferative potential of WS iPSCs after long-term culture

To determine whether reprogramming provides WS cells with infinite proliferative potential, we generated iPSCs from WS patient fibroblasts. Morphologically distinct colonies from parental cells emerged after transduction of Yamanaka factors using retroviruses and showed elevated alkaline phosphatase activity (Figures S1A and S1B). Colonies were picked up, and 6 WS iPSC lines were established using fibroblasts from 2 independent WS patients after several passages. In western blotting analysis using an anti-WRN antibody, WRN protein was not detected in WS iPSCs but was expressed in both normal fibroblasts and iPSCs (Figure S2A). Direct sequencing analysis of WS iPSCs identified compound heterozygous Mut4/Mut6 mutations in the *WRN* gene similar to those observed in parental cells, and the derivation of WS iPSCs from parental cells was confirmed by STR analysis (Figures S2B and S2C). Finally, the 6 WS iPSC lines #23, #34, and #64 from A0031 and #02, #13, and#14 from WSCU01 were successfully established.

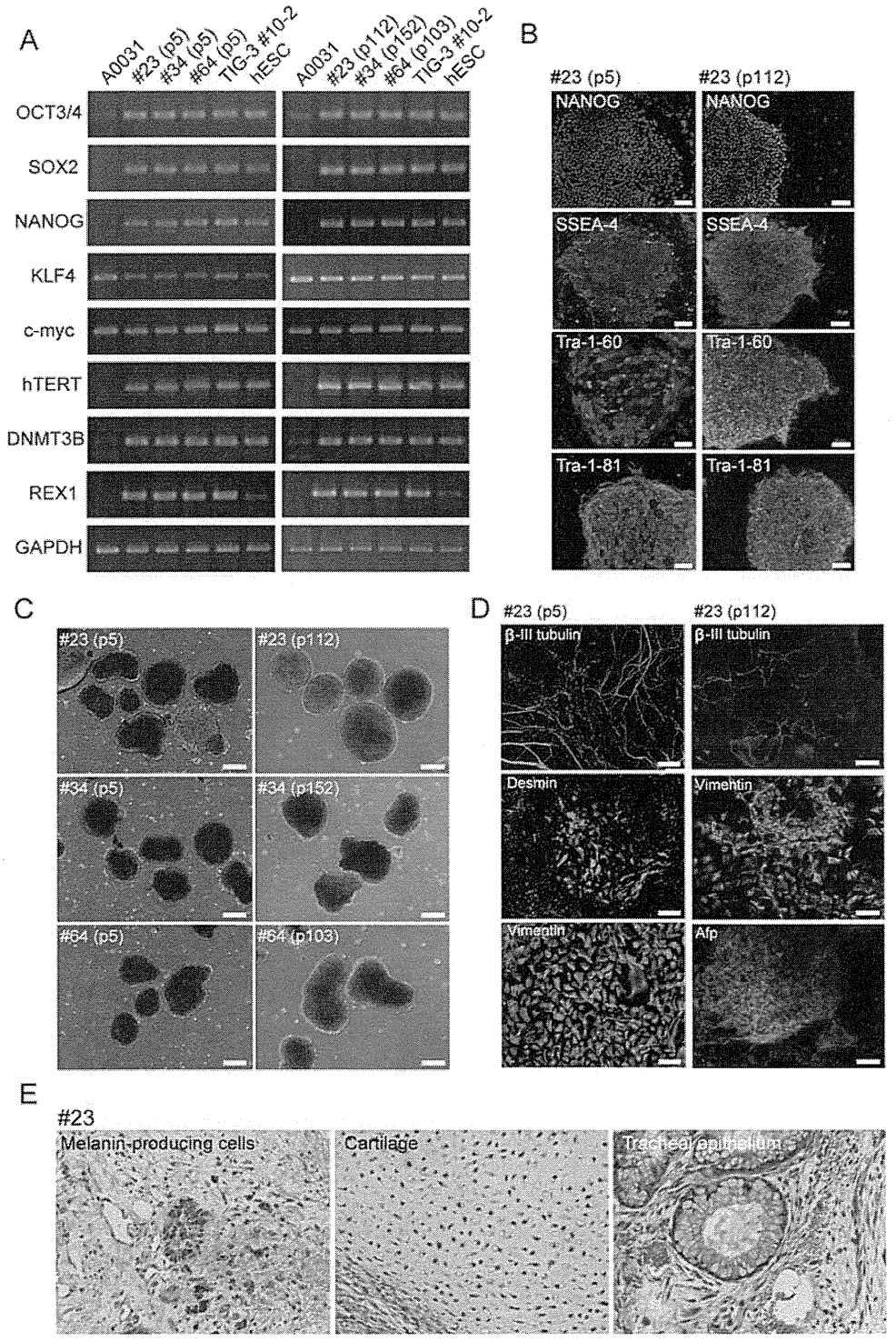

Figure 2. Sustained ESC-like characteristics of WS iPSCs after Long-Term Culture. (A) Expression of pluripotency genes in A0031-derived WS iPSC clones in early and late passages. (B) Expression of hESC markers in A0031-derived WS iPSC clone #23 in early and late passages. Bars = 100 μm. (C) EB formation in A0031-derived WS iPSC clones from early and late passages. Bars = 100 μm. (D) Immunocytochemical analysis of differentiation of EBs into 3 germ layers for A0031-derived iPSC clone #23 in early and late passages. β-III tubulin (ectoderm), desmin (mesoderm), vimentin (mesoderm and parietal endoderm), and α-fetoprotein (Afp, endoderm). Bars = 100 μm. (E) Hematoxylin and eosin histology of teratomas from A0031-derived iPSC clone #23. Formation of all 3 germ layers is shown including melanin-producing cells (ectoderm), cartilage (mesoderm), and tracheal epithelium (endoderm).
doi:10.1371/journal.pone.0112900.g002

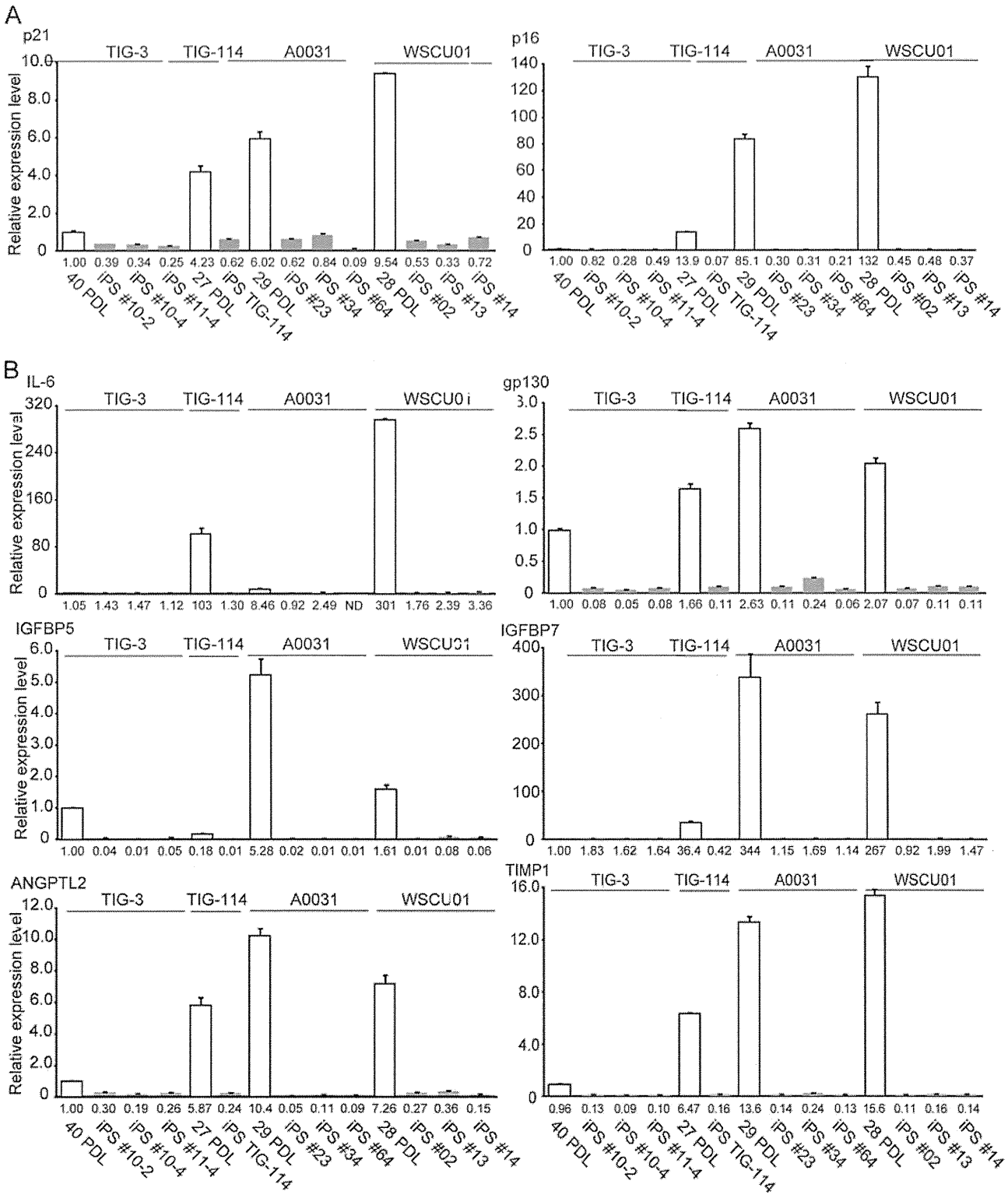

Figure 3. Suppression of Senescence-Associated Gene Expression in Reprogrammed WS iPSCs. (A) Expression of CDKI genes in parental fibroblasts and iPSCs. White columns show relative expression levels in the parental fibroblasts TIG-3, TIG-114, A0031, and WSCU01, and gray columns show those of their derived iPSC clones. Numbers under the horizontal axis in each graph show relative values in mRNA expression compared with that in TIG-3 fibroblasts. Values represent means of three technical replicates ± SD. (B) Expression of SASP genes in parental fibroblasts and iPSCs. Each graph is shown as in (A).
doi:10.1371/journal.pone.0112900.g003

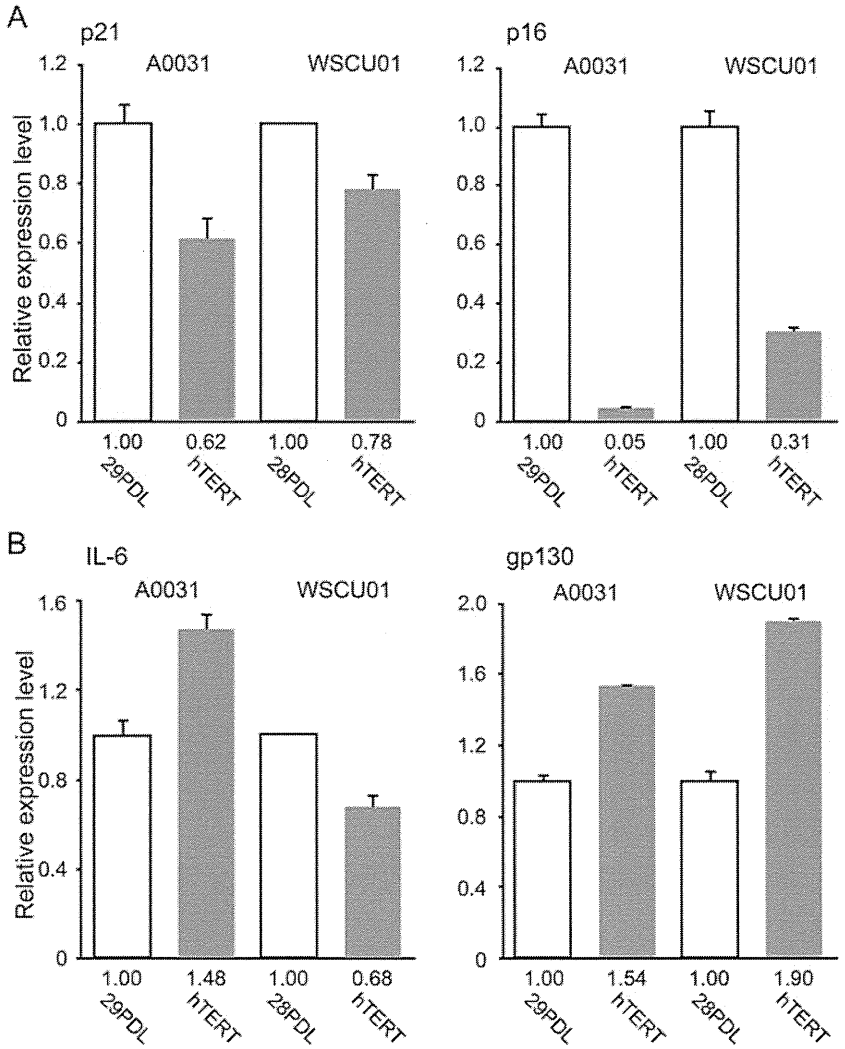

Figure 4. Reprogramming of the SASP gene loci is mediated by factors other than activated telomerase. (A) Expression of CDKI genes in WS fibroblasts and their hTERT-transduced derivatives. White columns show relative expression levels in A0031 and WSCU01 fibroblasts, and gray columns show those of their hTERT-transduced derivatives. Numbers under the horizontal axis in each graph show relative values in mRNA expression compared with that in parental fibroblasts. Values represent means of three technical replicates ± SD. (B) Expression levels of SASP genes in WS fibroblasts and their hTERT-transduced derivatives. Each graph is shown as in (C).
doi:10.1371/journal.pone.0112900.g004

WS iPSC lines from A0031 were cultured for 120 continuous passages over 2 years without morphological changes or loss of growth capacity (Figures 1A and 1B). Moreover, iPSC lines from WSCU01 proliferated for a year (Figures 1A and S1C). Average terminal restriction fragment (TRF) lengths in clones #23, #34, and #64 (A0031) were decreased, invariable, and increased during long-term culture, respectively, and similar telomere dynamics were observed in WSCU01-derived iPSC clones (Figure 1C).

Sustained ESC-like characters of WS iPSCs after long-term culture

To determine the persistence of ESC-like characteristics in WS iPSCs, we compared undifferentiated states and differentiation potentials between WS iPSCs from early and late passages. WS iPSC lines expressed pluripotency genes and hESC-specific surface markers during early passages (around p10), and during late passages (around p100; Figures 2A, 2B, S3 and S4). These iPSC lines also showed sustained formation of embryoid bodies and differentiation into 3 germ layers (Figures 2C, 2D, and S5). Furthermore, at around p50, WS iPSC lines generated teratomas that contained tissue structures of all 3 germ layers. These were consistent with those shown in normal iPSC lines after transplantation into the testes of SCID mice (Figures 2E and S6). Thus, reprogrammed WS fibroblasts acquired infinite proliferative potential, and the ESC-like characteristics of the resulting iPSCs were maintained for more than 2 years.

Suppression of senescence-associated gene expression in WS iPSCs after long-term culture

Global gene expression analysis using DNA chips showed pronounced similarities among pluripotent stem cells including WS iPSCs. However, marked differences between WS iPSC and WS fibroblasts were observed (Figure S7). Heat map analysis also showed a high analogy of global gene expression profiles in these

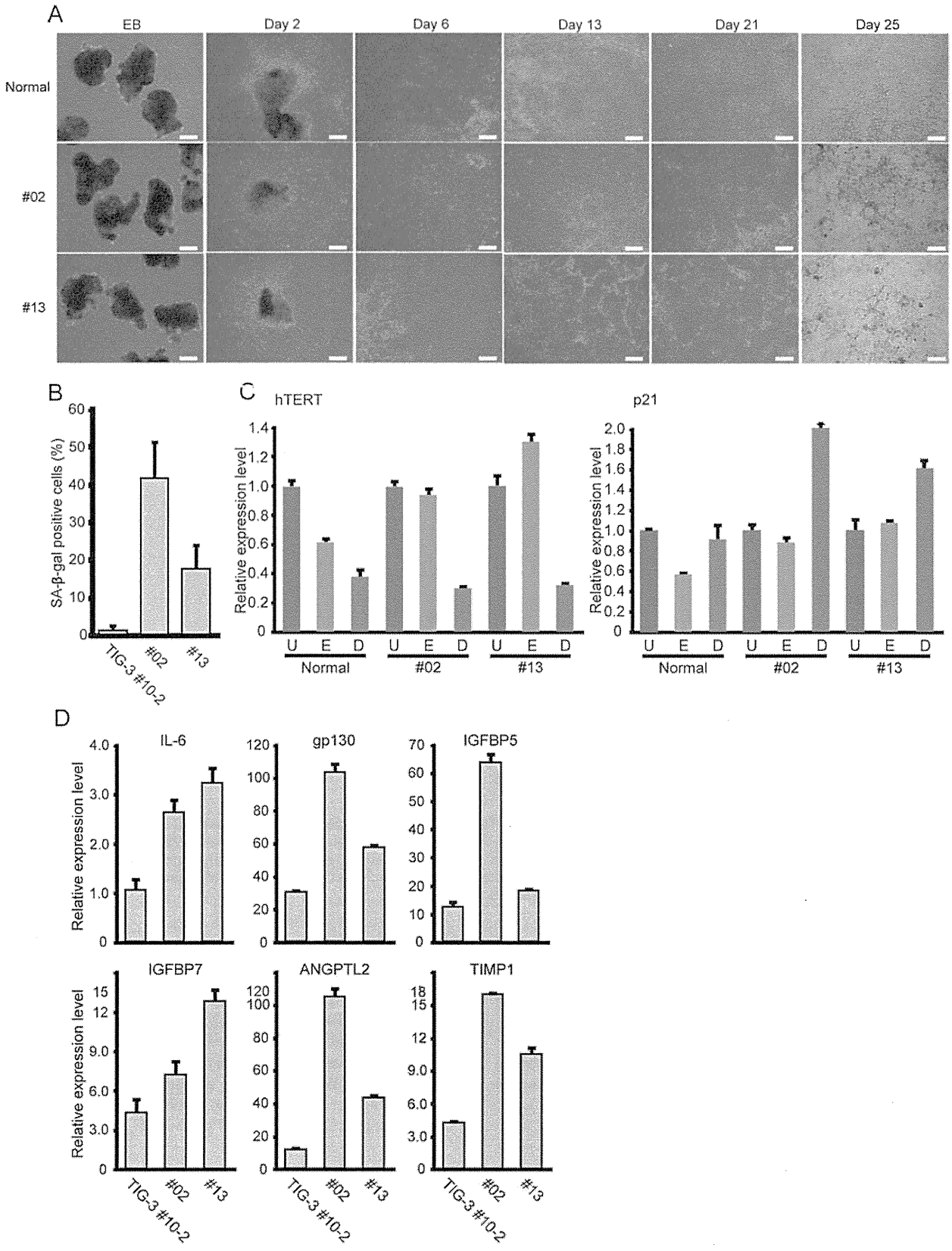

Figure 5. Recapitulation of Premature Senescence Phenotypes in Differentiated Cells from WS iPSCs. (A) Differentiation of EBs from normal (TIG-3) and WS (WSCU01 #02 and #13) iPSCs. Differentiated cells from WS iPSCs showed premature senescence. SA-β-gal staining was performed on day 25 of differentiation. Bars = 100 μm. (B) Percentage of senescent cells after 25 days of differentiation. SA-β-gal-positive cells were

counted in three randomly selected fields with 40× magnification. Values represent means of the three fields ± SD. (C) Expression of hTERT and p21 mRNAs in undifferentiated iPSCs ("U," red columns), EBs after 12 days of formation ("E," green columns), and differentiated cells after 25 days of differentiation ("D," blue columns). Values represent means of three technical replicates ± SD. (D) Expression of SASP genes in differentiated cells from normal (TIG-3) and WS (WSCU01 #02 and #13) iPSCs after 25 days of differentiation. Graphs shows fold changes relative to undifferentiated iPSCs. Values represent means of three technical replicates ± SD.
doi:10.1371/journal.pone.0112900.g005

pluripotent stem cell lines, but distinctly different profiles from those of WS fibroblasts (Figures S8A). Recent studies of aging have identified senescence-induced inflammatory and secretory factors that are collectively referred to as the senescence-associated secretory phenotype (SASP) and are the hallmarks of aging. It is widely accepted that age-associated inflammatory responses contribute to human aging mechanisms [26]. Accordingly, we observed downregulation of SASP secretory factors, including inflammatory cytokines, growth factors and MMPs, in both normal and WS iPSCs compared with WS fibroblasts (Figures S8B). Subsequently, we performed real-time qRT-PCR analysis using PDL-matched normal and patient fibroblasts, and their iPSC derivatives which were maintained in long-term culture. Although relative expression levels of the senescence-associated cyclin-dependent kinase inhibitor (CDKI) genes *p21Waf1/Cip1* and *p16INK4a* in normal fibroblasts correlated with the donor age, the expression levels of these genes were higher in WS fibroblasts than in normal fibroblasts, indicating that replicative senescence was prematurely induced in WS cells (Figure 3A). However, expression levels of these genes were significantly reduced in all iPSC clones from normal and WS cells (Figure 3A), suggesting that these gene loci are reprogrammed to the same degree in normal and WS iPSCs. Thus, we examined the expression of the typical SASP genes *IL-6* and *gp130* [27] and found higher expression levels in WS fibroblasts than in normal fibroblasts (Figure 3B). Moreover, expression levels of these genes drastically decreased in both normal and WS iPSCs compared with parental fibroblasts. Similarly, expression levels of the SASP genes *IGFBP5*, *IGFBP7*, *ANGPTL2*, and *TIMP1* ([28–31] were significantly decreased in both normal and WS iPSCs compared with parental fibroblasts (Figures 3B).

Reprogramming of the SASP gene loci is mediated by factors other than activated telomerase

WS fibroblasts were previously shown to bypass premature senescence following introduction of the telomerase gene *hTERT* [32], Similarly, the present WS cells bypassed premature replicative senescence, and hTERT allowed cell division for over 150 PDL in A0031 cells, and 40 PDL in WSCU01 cells compared with parental cells that became senescent at less than 30 PDL (Figures S9A and S9B). TRF length analysis showed that hTERT-expressing WS cells acquired longer telomeres during passages than parental cells (Figures S9C). To examine whether the expression of hTERT was sufficient to suppress the upregulation of aging-associated genes in WS cells, we compared expression levels of CDKI and SASP genes between WS fibroblasts and their hTERT-expressing derivatives. Whereas a decline in p21waf1/cip1 and p16INK4a mRNA expression was observed in hTERT-expressing cells (Figure 4A), IL-6 and gp130 expression was not suppressed following the introduction of hTERT, suggesting that reprogramming of the SASP gene loci is mediated by factors other than activated telomerase (Figure 4B). The present data show complete suppression of premature senescence phenotypes in WS cells using transcription factor-induced reprogramming and suggest that persistence of the undifferentiated state and pluripotency are crucial for reversing the aging process.

Recapitulation of premature senescence phenotypes in differentiated cells from WS iPSCs

To establish cell lineages that prematurely senesced, EBs consisting of equal numbers of iPSCs maintained in long-term culture were differentiated in serum-containing medium. Differentiated cells from WS iPSC-derived EBs were outgrown less rapidly than those from normal iPSC-derived EBs (Figure 5A, Day 2). These cells exhibited flat and enlarged morphology (Figure 5A, Day 6, 13, and 21) and became positive for SA-β-gal staining (Figure 5A, Day 25, and Figure 5B). Whereas expression levels of hTERT were downregulated equally in differentiated cells from normal and WS iPSCs, p21 mRNA was more highly induced in differentiated cells from WS iPSCs than those from normal iPSCs (Figure 5C). Expression levels of the SASP genes were also significantly increased in differentiated cells from WS iPSCs

Table 1. Results of chromosome analysis of WS iPSC clones and their parenral cells.

Cell lines	Numbers of cells analyzed by G-banding	Numbers of cells analyzed by M-FISH	Karyotypes
A0031	20 (13/7)	ND	46,XY,del(8)(q22q24)/46,XY,t(1;14)(p34.1;q13),t(4;7)(p15.2;q22),del(8)(q22q24)
iPS#23	20	10	46,XY,t(1;14)(p34.1;q13),t(4;7)(p15.2;q22),del(8)(q22q24),der(21)t(17;21)(?;q22.3)
iPS#34	20	10	46,XY,t(1;14)(p34.1;q13),t(4;7)(p15.2;q22),del(8)(q22q24)
iPS#64	20	10	46,XY,t(1;14)(p34.1;q13),t(4;7)(p15.2;q22),del(8)(q22q24),der(19)t(2;19)(?;p13.3)
WSCU01	20	ND	46,XY,normal
iPS#02	20	10	47,XY,+del(20)(p?)
iPS#13	20	10	46,XY,normal
iPS#14	20	10	46,XY,normal

Abbreviations: t, translocation; del, deletion; der, derivative chromosome; p, short arm; q, long arm.
doi:10.1371/journal.pone.0112900.t001

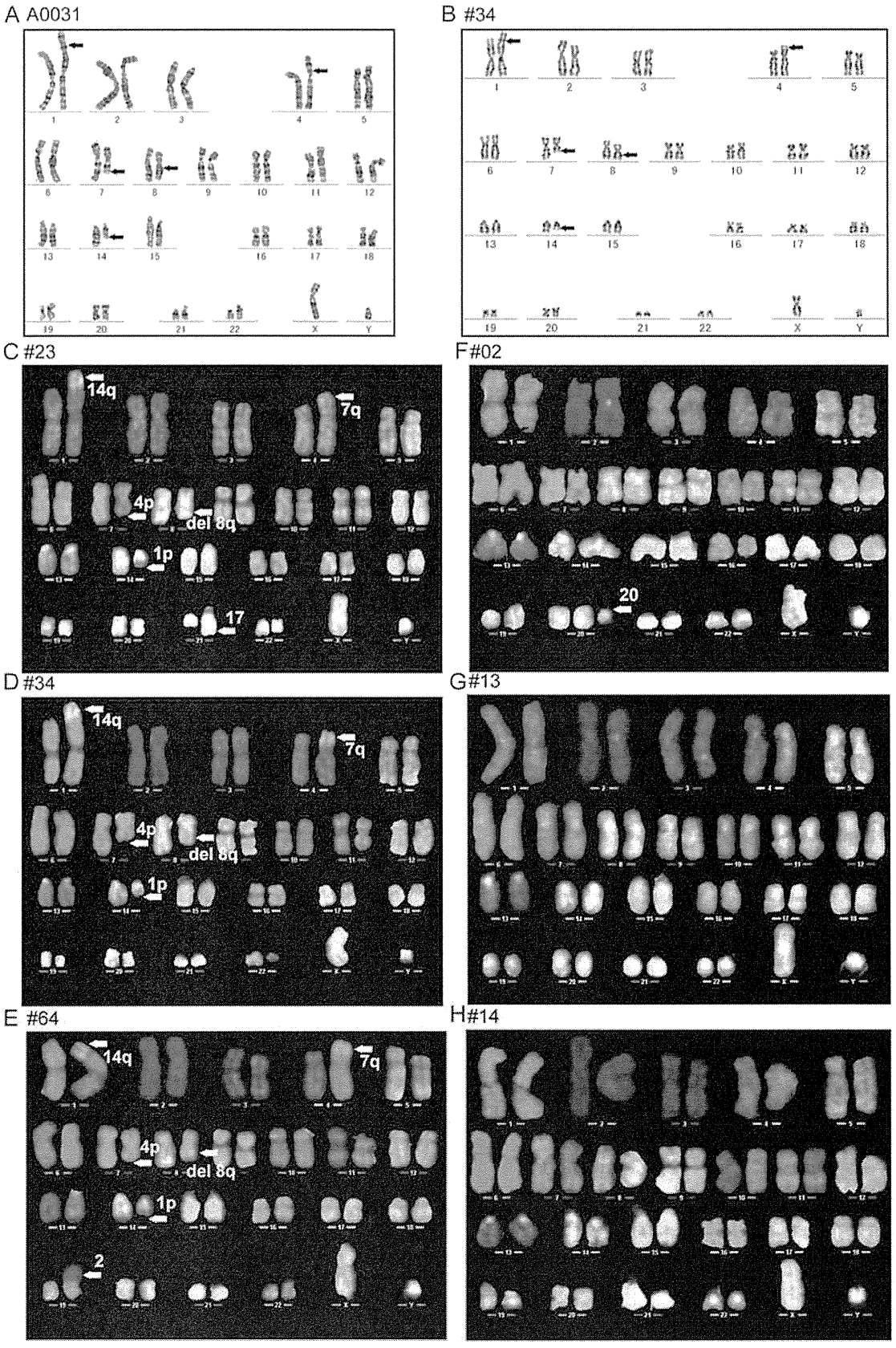
A A0031
B #34
C #23
14q
7q
4p
del 8q
1p
17
F#02
20
D #34
14q
7q
4p
del 8q
1p
G#13
E #64
14q
7q
4p
del 8q
1p
2
H#14

Figure 6. Karyotype Analysis of WS iPSCs. Chromosomal profiles of G-band analysis. (A) Parental A0031 fibroblast and (B) A0031-derived iPSC clone #34. Arrows indicate translocation breakpoints. Chromosomal profiles of M-FISH analysis. A0031-derived iPSC clones (C) #23, (D) #34, and (E) #64 and WSCU01-derived iPSC clones (F) #02, (G) #13, and (H) #14. Arrows indicate translocation breakpoints or an extra chromosome.
doi:10.1371/journal.pone.0112900.g006

compared with those from normal iPSCs (Figure 5D). These results demonstrated recapitulation of premature senescence phenotypes with downregulation of hTERT in differentiated cells from WS iPSCs.

Karyotype analysis of WS iPSCs

WS is characterized by genomic instability, and gene translocation events have been observed during culture of patient-derived cells [33]. Because reprogramming of somatic cells and subsequent maintenance of iPSCs involves extensive cell division, WS iPSCs may acquire additional chromosomal abnormalities. Thus, we compared chromosomal profiles of long-term cultured WS iPSC clones with those of parental WS fibroblasts by karyotype analysis. The subsequent G-banding stain and multicolor fluorescence *in situ* hybridization (M-FISH) analysis are summarized in Table 1.

Chromosomal profiles of parental A0031 WS fibroblasts showed mosaicism with the following abnormal karyotypes: 46, XY with a deletion in 8q and 46, XY with a deletion in 8q along with reciprocal translocations between 1p and 14q, and 4p and 7q (Figure 6A). These karyotypes support previous observations of chromosomal instability in WS cells [33]. Whereas, 1 of the derived iPSC clones (#34) had the same chromosomal profile as its parent cells (Figures 6B and 6D), the other 2 A0031-derived iPSC clones (#23 and #64) had the translocations 21q and 19p, respectively, in addition to those of the parental karyotype (Table 1, Figures 6C and 6E). Moreover, whereas parental WSCU01 fibroblasts and 2 of their derived iPSC clones (#13 and #14) had normal karyotypes (Table 1, Figures 6G and 6H), the remaining iPSC clone #02 carried the abnormal karyotype 47 (XY with an additional aberrant chromosome derived from chromosome 20; Table 1, Figure 6F).

The observation that 3 of 6 WS iPSC clones had the same karyotypes as their parental cells after approximately 100 passages suggests that karyotypes of WS cells are stabilized following reprogramming.

Discussion

In this study, we demonstrated that WS fibroblasts could be reprogrammed into iPSCs using Yamanaka factors, and the resulting iPSCs showed unlimited proliferative capacity that was sufficient for self-renewal over a period of 2 years. WS iPSCs also exhibited undifferentiated states and differentiation potential after long-term culture. Subsequently, we showed that WS iPSCs maintain immortality and ESC-like characteristics that indicate corrected telomere dysfunction following reprogramming of WS cells. Although WRN was not essential for generation of iPSCs, WRN helicase may protect genome integrity by mechanism other than the maintenance of telomere in iPSCs.

TRF length analysis indicated that WS iPSC lines maintained telomere with size variation in each clone. It is known that human iPSCs derived from normal somatic cells showed varied telomere length, and variation of telomere length among human iPSC clones is thought to partly depend on acquired telomerase activity associated with their reprogrammed states [34,35]. Therefore, variation of telomere length observed among WS iPSC clones would be due to clonal variation in telomerase activity rather than telomere dysfunction associated with *WRN* deficiency.

Normal human iPSCs are known to acquire genomic instability with a high incidence of additions, deletions and translocations [36,37]. In contrast, chromosomal aberrations are frequently caused by telomere dysfunctions in WS fibroblasts following the induction of cell cycle progression [11]. Nonetheless, the present data show unexpected maintenance of chromosomal profiles in WS iPSC clones during long-term culture for more than 100 passages although half of these clones acquired additional chromosomal abnormalities. Previously, the introduction of hTERT reduced the chromosomal aberrations in cells from WS patients [11]. In agreement, the present data indicate endogenous hTERT expression in WS iPSCs, but not in parental fibroblasts, suggesting that reprogramming suppresses chromosomal instability in WS cells by reactivating telomerase.

Previous studies show that WS fibroblasts express inflammatory cytokines [38] and WS is associated with inflammatory conditions such as atherosclerosis, diabetes and osteoporosis [39–43]. The present data indicate that both CDKI and SASP genes are prematurely induced in WS fibroblasts compared with PDL-matched normal fibroblasts. However, expression levels of these genes were completely suppressed in WS iPSCs to the same degree observed in normal iPSCs. In contrast, hTERT did not suppress SASP genes in WS fibroblasts, as shown by previous study [44], although a decline in p21waf1/cip1 and p16INK4a mRNAs was observed. Taken together, these observations suggest that pluripotency-associated transcription factor-induced reprogramming reverses the aging process in both normal and WS cells. Furthermore, differentiated cells from EBs of long-term cultured WS iPSCs showed premature senescence phenotypes, thus demonstrating that WS iPSCs stably maintained their potential to recapitulate premature senescence phenotypes during differentiation over the long term. In addition, embryoid body-mediated iPSC differentiation recapitulated premature senescence phenotypes in WS iPSCs, suggesting that it would provide a simple and rapid way to identify cell lineages affected in WS.

In the present study, we demonstrated the potential of WS iPSCs to proliferate infinitely and differentiate into various cell types, which could be used to provide patient cells in large quantities over the long term. Because WS-specific iPSCs may be differentiated into multiple cell types, their experimental use may resolve the major pathogenic processes of WS for which cell types available from patients are usually limited to lymphocytes and/or fibroblasts. The present technologies may also be used to develop cell transplantation therapies for WS patients using gene-corrected patient cells. The present observations indicate that WS iPSCs may be a powerful tool for understanding normal aging and the pathogenesis of WS.

Supporting Information

Figure S1 Generation of WS iPSCs. (A) Generation of iPSCs. Normal (TIG-3) and Werner syndrome (A0031 and WSCU01) fibroblasts are shown in the left panels, and emergence of morphologically distinct ESC-like colonies from parental cells is shown in the right panels. (B) Alkaline phosphatase activity of ESC-like colonies derived from TIG-3 and A0031 fibroblasts. (C) Colony morphologies of WSCU01-derived WS iPSC clones in early and late passages. Bars = 100 μm.
(EPS)

Figure S2 Evidences that WS iPSCs were derived from patients. (A) Western blot analysis of WRN helicase protein in WS iPSCs. (B) Direct sequencing analysis identified compound heterozygous mut.4/mut.6 mutations in WS iPSCs. Mut.4 is a C to G substitution at the splice-donor site bordered by exon 26, as shown by an arrow in the illustration of the double-strand base sequence. Obtained pherograms show antisense peak shapes. A peak corresponding to mut.4 in normal TIG-3 fibroblast shows a single "C," whereas the WS iPSC clone #34 from A0031 fibroblasts gave double peaks showing "G" in addition to "C." Mut.6 is a T to C substitution in exon 9. A peak corresponding to mut.6 in normal cells showed a single "C," whereas WS iPSC gave double peaks showing "T" in addition to "C." C, blue; G, black; T, red; A, green. (C) STR analysis of A0031-derived iPSC clone #34, showing that iPSC clone #34 was derived from the parental A0031 fibroblasts.
(EPS)

Figure S3 Expression of pluripotency genes in WSCU01-derived WS iPSC clones in early and late passages.
(EPS)

Figure S4 Expression of hESC markers in WS iPSCs in early and late passages. A0031-derived clones #34, and #64, and WSCU01-derived clones #02, #13, and #14 are shown. Bars = 100 μm.
(EPS)

Figure S5 Immunocytochemistry for differentiation of embryoid bodies into 3 germ layers for WS iPSCs in early and late passages. A0031-derived clones #34, and #64, and WSCU01-derived clones #02, #13, and #14 are shown. Bars = 100 μm.
(EPS)

Figure S6 Hematoxylin and eosin histology of teratomas derived from iPSCs. Hematoxylin and eosin histology of teratomas derived from iPSCs. The normal TIG-3 fibroblast-derived clone #10-2, A0031-derived clones #34, and #64, and the WSCU01-derived clone #02 are shown. Formation of all 3 germ layers is shown with melanin-producing cells and glial tissue (ectoderm), cartilage (mesoderm) and intestinal epithelia. Glands are lined by columnar epithelia and tracheal epithelium (endoderm).
(EPS)

Figure S7 Figure Scatter plots comparing gene expression profiles.
(EPS)

Figure S8 Analysis of senescence-associated gene expression in iPSCs. (A) Heat map analysis of WS iPSC #34 and parental WS A0031 fibroblasts, normal TIG-3 fibroblast-derived iPSCs, and hESC; 3277 probes with >5-fold differences in expression between A0031 fibroblast and WS iPSC were included in the heat map. (B) Heat map analysis of the gene profiles of secreted protein probes with >2-fold differences in expression between A0031 fibroblasts and the 3 pluripotent stem cell lines WS iPSC, TIG-3 iPSC, and hESC.
(EPS)

Figure S9 hTERT bypassed premature replicative senescence of WS fibroblasts. (A) Morphologies of growing normal TIG-3 fibroblasts, and A0031 and WSCU01 WS fibroblasts. WS fibroblasts showed premature senescence. SA-β-gal staining was performed for WSCU01 (lower). Bars = 100 μm. (B) Cumulative population doubling levels for hTERT-expressing WS cells. (C) TRF lengths of A0031 fibroblasts and their TERT-transduced derivatives.
(EPS)

Table S1
(EPS)

Table S2
(EPS)

Acknowledgments

We are grateful to Miho Kusuda-Furue (National Institute of Biomedical Innovation), Hidenori Akutsu (National Center for Child Health and Development) and Haruhiko Koseki (RCAI RIKEN) for their help, encouragement and suggestions. We also thank M. K. F and Bunsyo Shiotani for the critical review of draft manuscripts, and the Analysis Center of Life Science, Natural Science Center for Basic Research and Development of Hiroshima University for processing microarray data.

Author Contributions

Conceived and designed the experiments: AS. Performed the experiments: AS HK KZ YS YK MO MO HK TS KH HS YI KH YK. Analyzed the data: AS YK MO MO TS KH HS YI KH YK. Contributed reagents/materials/analysis tools: MG MT KY SY KF HT. Wrote the paper: AS MG. Final approval of the version to be published: AS HT.

References

1. Goto M, Miller RW, Ishikawa Y, Sugano H (1996) Excess of rare cancers in Werner syndrome (adult progeria). Cancer Epidemiol Biomarkers Prev 5: 239–246.
2. Goto M (2000) Werner's syndrome: from clinics to genetics. Clin Exp Rheumatol 18: 760–766.
3. Salk D, Au K, Hoehn H, Martin GM (1981) Effects of radical-scavenging enzymes and reduced oxygen exposure on growth and chromosome abnormalities of Werner syndrome cultured skin fibroblasts. Hum Genet 57: 269–275.
4. Yu CE, Oshima J, Fu YH, Wijsman EM, Hisama F, et al. (1996) Positional cloning of the Werner's syndrome gene. Science 272: 258–262.
5. Oshima J, Yu CE, Piussan C, Klein G, Jabkowski J, et al. (1996) Homozygous and compound heterozygous mutations at the Werner syndrome locus. Hum Mol Genet 5: 1909–1913.
6. Goto M, Imamura O, Kuromitsu J, Matsumoto T, Yamabe Y, et al. (1997) Analysis of helicase gene mutations in Japanese Werner's syndrome patients. Hum Genet 99: 191–193.
7. Matsumoto T, Imamura O, Yamabe Y, Kuromitsu J, Tokutake Y, et al. (1997) Mutation and haplotype analyses of the Werner's syndrome gene based on its genomic structure: genetic epidemiology in the Japanese population. Hum Genet 100: 123–130.
8. Shimamoto A, Sugimoto M, Furuichi Y (2004) Molecular biology of Werner syndrome. Int J Clin Oncol 9: 288–298.
9. Rossi ML, Ghosh AK, Bohr VA (2010) Roles of Werner syndrome protein in protection of genome integrity. DNA Repair (Amst) 9: 331–344.
10. Crabbe L, Verdun RE, Haggblom CI, Karlseder J (2004) Defective telomere lagging strand synthesis in cells lacking WRN helicase activity. Science 306: 1951–1953.
11. Crabbe L, Jauch A, Naeger CM, Holtgreve-Grez H, Karlseder J (2007) Telomere dysfunction as a cause of genomic instability in Werner syndrome. Proc Natl Acad Sci U S A 104: 2205–2210.
12. Takahashi K, Yamanaka S (2006) Induction of pluripotent stem cells from mouse embryonic and adult fibroblast cultures by defined factors. Cell 126: 663–676.
13. Takahashi K, Tanabe K, Ohnuki M, Narita M, Ichisaka T, et al. (2007) Induction of pluripotent stem cells from adult human fibroblasts by defined factors. Cell 131: 861–872.
14. Yu J, Vodyanik MA, Smuga-Otto K, Antosiewicz-Bourget J, Frane JL, et al. (2007) Induced pluripotent stem cell lines derived from human somatic cells. Science 318: 1917–1920.
15. Aoi T, Yae K, Nakagawa M, Ichisaka T, Okita K, et al. (2008) Generation of pluripotent stem cells from adult mouse liver and stomach cells. Science 321: 699–702.
16. Stadtfeld M, Hochedlinger K (2010) Induced pluripotency: history, mechanisms, and applications. Genes Dev 24: 2239–2263.